

# Transport Properties of the Ionic Liquid 1-Ethyl-3-Methylimidazolium Chloride from Equilibrium Molecular Dynamics Simulation. The Effect of Temperature

Carlos Rey-Castro\* and Lourdes F. Vega

*Institut de Ciència de Materials de Barcelona (ICMAB-CSIC), Consejo Superior de Investigaciones Científicas, Campus de la UAB, 08193 Bellaterra, Spain*

*Received: May 11, 2006*

We present here equilibrium molecular dynamics simulation results for self-diffusion coefficients, shear viscosity, and electrical conductivity in a model ionic liquid (1-ethyl-3-methylimidazolium chloride) at different temperatures. The Green–Kubo relations were employed to evaluate the transport coefficients. When compared with available experimental data, the model underestimates the conductivity and self-diffusion, whereas the viscosity is overpredicted, showing only a semiquantitative agreement with experimental data. These discrepancies are explained on the basis of the rigidity and lack of polarizability of the model. Despite this, the experimental trends with temperature are remarkably well reproduced, with a good agreement on the activation energies when available. No significant deviations from the Nernst–Einstein relation can be assessed on the basis of the statistical uncertainty of the simulations, although the comparison between the electric current and the velocity autocorrelation functions suggests some degree of cross-correlation among ions in a short time scale. The simulations reproduce remarkably well the slope of the Walden plots obtained from experimental data of 1-ethyl-3-methylimidazolium chloride, confirming that temperature does not alter appreciably the extent of ion pairing.

## 1. Introduction

Room-temperature ionic liquids (RTILs or, simply, ILs) are a group of organic salts with melting points below 100 °C. These substances are receiving increasingly greater attention on account of their application as alternative solvents due to their physicochemical properties. Among other interesting features, ILs show negligible vapor pressures, high thermal stabilities and ionic conductivities, and a wide temperature range in the liquid state. Besides, ILs are nonflammable, and they usually display a good solvent ability toward a wide range of solutes. All these properties compare positively with most conventional organic solvents.<sup>1–5</sup> In addition, ILs present an enormously large number of chemical compositions, with a virtually infinite number of possible ion pair combinations. Typically, ILs consist of a large organic cation with low symmetry (most often differently substituted imidazolium, pyridinium, and quaternary ammonium or phosphonium ions) combined with an enormously wide range of anions, usually of smaller size. Accordingly to their composition complexity, these substances offer a very wide range of thermophysical properties. This has led to the concept of ILs as “tailor-made” or “designer” solvents for specific applications.

Among all physical properties of ILs, transport properties such as viscosity, self-diffusion, and electric conductivity are particularly important parameters that must be accounted for in the selection of a given IL for its applications as an alternative solvent or conductor. ILs present relatively high viscosities, normally on the same order of magnitude as those of oils. This poses a limitation to some of their possible applications. For instance, a low viscosity would be desirable in order to enhance mass transfer in two-phase separation processes with ILs; the relatively long equilibration times in the absorption of gases by ILs are a consequence of the low diffusivity of the solutes on a highly viscous medium.<sup>6</sup> The transport properties are also

crucial when considering the reaction kinetics in a synthetic process or ion transport in an electrochemical device. Regarding the important role of ILs as reaction media, the significance of transport properties is manifested, among other things, in the fact that chemical reactions can be diffusion-limited even for highly soluble molecules.<sup>1,7</sup> In fact, most of current research for the development of new and more useful ILs is focused on the synthesis of products with improved transport properties (low viscosity, high electrical and heat conductivities, etc.).

The basic features of the experimental behavior of the transport properties in ILs have been reviewed in the recent literature.<sup>1–4,7–9</sup> Regarding the effect of temperature, a marked decrease in viscosity and increase in both conductivity and self-diffusion with temperature is observed in all cases. The three properties usually exhibit a classical linear Arrhenius behavior above room temperature, with deviations from the linear trend in the proximities of the glass transition temperatures, which are best described through the empirical Vogel–Tamman–Fulcher (VTF) equation.<sup>1,10,11</sup> The temperature dependence of the transport properties is a result of the complex interplay of short- and long-range forces between ions, and it is still not well-understood from a theoretical point of view.

Despite its relevance for the chemical reactivity, rheology, electrical conductivity, and mass transfer processes involving ILs, the correlation between chemical structure and transport properties in ILs is still not completely understood. The transport behavior of room-temperature molten salts is determined by the collective dynamics of their ionic constituents, i.e., the cations and the anions. A reliable approach to this collective motion can be provided by molecular dynamics (MD) simulation using an adequate molecular model. The comparison of simulations with experimental data allows us to analyze the relationship between molecular parameters and macroscopic transport properties.

A revision of molecular modeling studies of bulk ILs, beginning from the seminal work of Hanke et al.,<sup>12</sup> has been

\* Corresponding author. crey@icmab.es.

recently published.<sup>13</sup> The force-field models for ionic liquids reported in bibliography so far have been reviewed by Canongia Lopes et al.<sup>14,15</sup> Despite the relatively large amount of experimental data on viscosities and electrical conductivities already available, the number of simulation studies attempting the calculation of these parameters is still scarce. The reason for this is the large computational effort required to sample these properties from equilibrium MD simulations. To mention some of the very few examples found in bibliography, shear viscosity estimates obtained from MD simulations have been reported for [mmim]Cl<sup>16</sup> and [emim]NO<sub>3</sub>.<sup>17</sup> To the best of our knowledge, no simulation study on the temperature effect on either viscosity or electrical conductivity has been published to date.

On the contrary, the self-diffusion coefficients of the ions can be calculated with relatively good statistical accuracy at less computational cost, and accordingly, several examples of estimates from MD simulations can be found in the bibliography.<sup>13</sup> In fact, the calculated diffusion coefficients are often employed to estimate the values of the viscosity<sup>18</sup> or the electrical conductivity<sup>19</sup> through Stokes or Nernst–Einstein relations, instead of carrying out their calculation directly from the corresponding correlation functions using Green–Kubo relationships.

The goal of this work is to analyze the effect of temperature on some of the most relevant transport coefficients in ILs, as well as their mutual relationships, by means of MD simulations. Notwithstanding the difficulty in the calculation of viscosities and electrical conductivities from MD simulations, it seems interesting to carry out a comparison with experimental behavior, searching for the experimental trends, and an analysis of the mutual relationships among the different transport coefficients. This study will provide additional insights about important aspects of the physical chemistry of ILs, such as the relevance of cation–anion correlations, or the link between local structure and dynamic behavior. This comparison can be proposed as a reference for the suggestion and validation of molecular force fields of ILs. Because one of the attractive features of the ILs is the extended temperature range of liquid-state behavior they offer, it is also important to understand the effect of temperature on the various transport properties. These are some of the issues addressed throughout this work.

For this purpose, equilibrium molecular dynamics simulations at different temperatures were performed for 1-ethyl-3-methylimidazolium chloride, [emim]Cl. There are several reasons for choosing this IL for this study: (1) The 1,3-dialkylimidazolium salts were the first ILs to be studied through molecular simulation,<sup>12</sup> and different sets of force field parameters have been developed and validated for them. (2) Moreover, among the ILs studied through simulation so far, [emim]Cl has the advantage of having a relatively simple, and yet asymmetric, cation and a monatomic anion, which entails comparatively less computational cost. (3) Finally, experimental data on transport properties of [emim]Cl are already available in the literature, enabling direct comparisons with the experimental systems.

The remainder of the paper is organized as follows: We revised the methodology used to calculate the transport properties, the molecular model, and the simulation details in section 2, while the main results and discussion are provided in section 2. Finally, some concluding remarks are given in section 4.

## 2. Methodology

**A. Calculation of Transport Coefficients.** The transport coefficients reported here were calculated through the corresponding Green–Kubo relations.<sup>20–23</sup> Within this formalism, the self-diffusion coefficient ( $D$ ) of each ion is calculated from its velocity autocorrelation function ( $vacf$ ) through the following

expression:

$$D = \frac{1}{3N} \int_0^\infty \sum_{i=1}^N \langle \vec{v}_i(t_0 + t) \cdot \vec{v}_i(t_0) \rangle dt \quad (1)$$

Here, the broken brackets  $\langle \dots \rangle$  represent the average over all time origins  $t_0$  within the trajectory,  $\vec{v}_i$  represents the velocity of the center of mass of particle  $i$  at any specific time, and  $t$  is the delay time of the correlation function. The velocity autocorrelation function is a single particle function, and therefore, the sum over all molecules in the system as well as the inclusion of the three velocity coordinates improves the statistics in the calculated coefficients.<sup>22</sup> In practical terms, the upper limit of the integral in eq 1 means that the integral must be calculated up to a point where the autocorrelation function decays to zero. In this work, an empirical exponential decay function has been fitted to the asymptotic part of the running integral in eq 1 in order to extrapolate the diffusion coefficients

$$D(t) = D + a \cdot \exp(-b \cdot t) \quad (2)$$

where  $D(t)$  is the running integral in eq 1, and  $a$ ,  $b$  are empirical fitting parameters. The statistical uncertainty is reported in this work as the standard deviation of the residues in  $D(t)$ .

The shear viscosity ( $\eta$ ) at zero shear rate is calculated from the integral over time of the pressure tensor autocorrelation function following the Green–Kubo relation

$$\eta = \frac{V}{k_B T} \int_0^\infty \langle P_{\alpha\beta}(t_0 + t) \cdot P_{\alpha\beta}(t_0) \rangle dt \quad (3)$$

Again, the brackets indicate that average must be taken over all time origins  $t_0$ ,  $V$  is the volume of the system,  $T$  is the temperature, and  $k_B$  is the Boltzmann constant.  $P_{\alpha\beta}$  denotes the element  $\alpha\beta$  of the pressure tensor. Unlike self-diffusion, the shear viscosity is a collective function, so it is not statistically improved by averaging over the number of particles in the system.<sup>22</sup> Some statistical improvement in the calculated shear viscosity can be achieved by averaging over six independent terms of the pressure tensor, namely,  $P_{xy}$ ,  $P_{yz}$ ,  $P_{zx}$ ,  $0.5(P_{xx} - P_{yy})$ ,  $0.5(P_{yy} - P_{zz})$ , and  $0.5(P_{xx} - P_{zz})$ .<sup>24</sup> The elements of the pressure tensor are calculated during the simulation using the following expression:<sup>22</sup>

$$P_{\alpha\beta} = \frac{1}{V} \left[ \sum_j m_j v_{\alpha j} v_{\beta j} + \frac{1}{2} \sum_{i \neq j} r_{\alpha i j} f_{\beta i j} \right] \quad (4)$$

where  $m_j$  is the mass of particle  $j$  and  $v_j$  is its velocity, while  $r_{ij}$  and  $f_{ij}$  represent, respectively, the distance and the force between particles  $i$  and  $j$ . The subscripts  $\alpha$  and  $\beta$  refer to the corresponding components of the vectors.

The integral in eq 3 is, in general, rather inaccurate for long times, especially for slowly decaying autocorrelation functions. In this work, an empirical double-decay exponential autocorrelation function is used to fit the running integral in eq 3 in order to obtain a reliable estimate of the viscosity.<sup>25</sup> The integration of such autocorrelation function yields

$$\eta(t) = A\alpha\tau_1(1 - e^{-t/\tau_1}) + A(1 - \alpha)\tau_2(1 - e^{-t/\tau_2}) \quad (5)$$

where  $A$ ,  $\alpha$  are empirical fitting parameters,  $0 < \alpha < 1$ , and  $\tau_1$ ,  $\tau_2$  are two characteristic decay times (usually differing by an order of magnitude). These parameters are obtained from the least-squares fit of eq 5 (weighted as  $1/t^2$ ). From them, an error estimate in the viscosity can be calculated using the following expression:<sup>25</sup>

$$\Delta\eta = \sqrt{\frac{2A[\alpha\tau_1 + (1-\alpha)\tau_2]}{t_{\max}}} \quad (6)$$

where  $t_{\max}$  is the maximum decay time considered in the calculation of the autocorrelation function.

The electrical conductivity ( $\sigma$ ) is calculated as the time integral of the electrical current autocorrelation function<sup>23</sup>

$$\sigma = \frac{1}{3k_BTV} \int_0^\infty \langle \vec{J}(t_0 + t) \cdot \vec{J}(t_0) \rangle dt \quad (7)$$

where the electrical current  $\vec{J}(t)$  is given by

$$\vec{J} = \sum_{i=1}^N q_i \vec{v}_i \quad (8)$$

and  $q_i$  represents the charge of ion  $i$ .

Like the shear viscosity, the electrical conductivity is a collective dynamical property and, for this reason, suffers from relatively high statistical uncertainty. Again, an exponential decay function was fitted to the long-time behavior of the integral of the autocorrelation function in order to obtain an extrapolated value of  $\sigma$ .

Preliminary molecular dynamic simulations with a simple model of molten salt were performed in order to test the procedures shown for the estimation of the transport properties. For this purpose, the classical potential model of Born–Huggins–Mayer for ion pair interactions in molten salts was employed

$$U = \sum_{i=1}^{N-1} \sum_{j>1}^N \left[ \frac{q_i q_j}{r_{ij}} + A_{ij} e^{B(\sigma_i + \sigma_j - r_{ij})} - \frac{C_{ij}}{r_{ij}^6} - \frac{D_{ij}}{r_{ij}^8} \right] \quad (9)$$

in combination with the parameters  $A_{ij}$ ,  $B$ ,  $\sigma_i$ ,  $C_{ij}$ , and  $D_{ij}$  determined for NaCl by Tosi and Fumi.<sup>26,27</sup> This classical model has been extensively used in simulations of molten salts, including the calculation of their transport properties. A good agreement has been obtained with bibliographic results of MD simulations using the same force field in similar conditions (see Figure 1 and Table 1).

**B. Molecular Model.** Equilibrium molecular dynamics simulations of the ionic liquid 1-ethyl-3-methylimidazolium chloride were performed using the model of Kim et al.<sup>28</sup> Although there are some discrepancies between experimental data and results obtained from this model, most of them explained on the basis of its rigidity and nonpolarizability, it still keeps most of the relevant features of ILs. This makes it a good choice as the starting point for a rigorous systematic analysis of the dependence of the transport properties of ILs with temperature, searching for general trends. It should be mentioned that our purpose is not to modify this force field nor to propose a new force field for [emim]Cl; on the contrary, we intend to check the accuracy of this available force field, used several times in the literature, for providing reliable transport

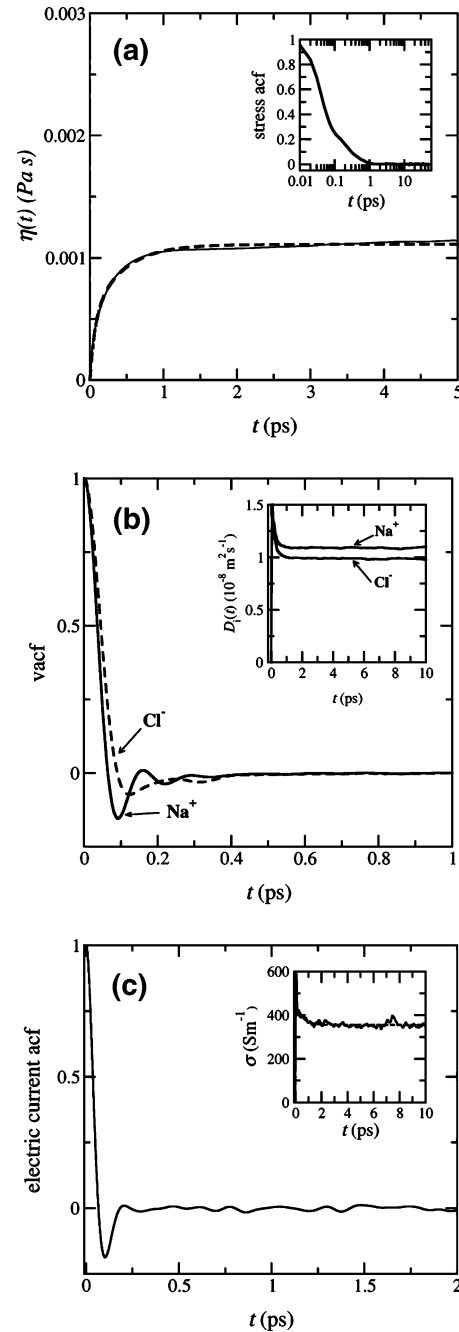


**Figure 1.** Transport properties of molten NaCl, calculated from equilibrium MD simulations using the Green–Kubo relationships: (a) shear viscosity at 1126 K; (b) self-diffusion of Na<sup>+</sup> and Cl<sup>−</sup> at 1305 K; (c) electrical conductivity at 1305 K.

properties as a function of temperature. Hence, results provided here are predictions obtained from the force field, without any refinement.

In the model of Kim et al.,<sup>28</sup> the united atom representation for the CH<sub>2</sub> and CH<sub>3</sub> groups is adopted. The cation is represented by a rigid body, and its geometry (bond lengths, angles) was

**TABLE 1: Transport Coefficients of Molten NaCl Obtained from Equilibrium MD Simulations Using the Born–Mayer–Huggins Model and the Green–Kubo Relations<sup>a</sup>**

$T$ (K)	$\eta$ (mPa s)	$T$ (K)	$\sigma$ (S cm <sup>−1</sup> )	$T$ (K)	$D_{\text{Na}^+}$ (10 <sup>−8</sup> m <sup>2</sup> s <sup>−1</sup> )	$D_{\text{Cl}^-}$ (10 <sup>−8</sup> m <sup>2</sup> s <sup>−1</sup> )
1126	1.11 ± 0.01 <sup>b</sup>	1305	3.6 ± 0.1 <sup>b</sup>	1305	1.090 ± 0.004 <sup>b</sup>	0.988 ± 0.004 <sup>b</sup>
1091	1.18 ± 0.01 <sup>c</sup>	1300	4.1 <sup>d</sup>	1300	1.12 <sup>d</sup>	1.03 <sup>d</sup>

<sup>a</sup> Comparison with simulation results from bibliography. <sup>b</sup> This work. <sup>c</sup> Galamba et al.<sup>51</sup> <sup>d</sup> Koishi et al.<sup>52</sup>

**TABLE 2: Temperatures, Molar Volumes, and Average Intermolecular Energies of the Systems Simulated in This Work**

$T$ (K)	$V_M^a$ (cm <sup>3</sup> /mol)	$U^b$ (kJ mol <sup>-1</sup> )	$U_{\text{Coul}}$ (kJ mol <sup>-1</sup> )
378	142.98	-508.4	-481.4
395	144.95	-506.1	-480.0
444	148.58	-501.2	-476.5
489	151.82	-497.0	-473.6

<sup>a</sup> The molar volume increases linearly with  $T$  with slope 0.078 cm<sup>3</sup> mol<sup>-1</sup> K<sup>-1</sup>. <sup>b</sup> Sum of Lennard-Jones and Coulombic potential energies.

taken from experimental X-ray diffraction data obtained from crystals of [emim]Br.<sup>29</sup> The electrostatic description of the cation consists of fixed partial charges centered on the atoms, following the assignments of Hanke et al.<sup>12</sup> The interaction potential in the system is represented by a sum of pairwise additive interatomic Lennard-Jones and Coulombic potentials

$$U = \sum_{i=1}^{N-1} \sum_{j>i}^N [U^{\text{LJ}}(r_{ij}) + U^{\text{Coul}}(r_{ij})] \quad (10)$$

with

$$U^{\text{LJ}}(r_{ij}) = 4\epsilon_{ij} \left[ \left( \frac{\sigma_{ij}}{r_{ij}} \right)^{12} - \left( \frac{\sigma_{ij}}{r_{ij}} \right)^6 \right] \quad (11)$$

and

$$U^{\text{Coul}}(r_{ij}) = \frac{q_i q_j}{4\pi\epsilon_0 r_{ij}} \quad (12)$$

The model of Kim et al. is based on the Amber force field for the Lennard-Jones (LJ) parameters of the individual atoms<sup>30</sup> and makes use of the conventional Lorentz–Berthelot combining rules. The chloride atom is represented by an LJ sphere with  $\sigma = 4.4$  Å and  $\epsilon/k_B = 50.4$  K carrying a unit negative charge. It must be mentioned that there is a relatively large uncertainty in the parametrization of the force field of most of the common anions in ILs, and of chloride ion in particular.<sup>14</sup> As far as the cation is concerned, the force field employed here is one of the simplest models found in bibliography,<sup>13</sup> since it does not account for any intramolecular degree of freedom or the electronic polarizability of the molecule. Despite this, the model still incorporates basic molecular features of [emim]Cl, such as size, cation asymmetry, and charge distribution. Concerning the latter, one can find in the bibliography a great variety of partial atomic charge assignments for imidazolium ions, which are usually proposed on the basis of ab initio calculations at different levels of theory. Despite this, the differences in the electrical dipole moments calculated from the different models are very small.<sup>31</sup>

**C. Simulation Details.** The simulated systems consisted of cubic boxes with periodic boundary conditions and 125 ion pairs (1500 atoms), although simulations of 64 and 216 ion pairs (768 and 2592 atoms) have also been performed in order to evaluate the possible influence of the system size. The starting configurations were simple cubic regular lattices. Initial MD simulations were performed in the NPT ensemble (using the Melchionna modification of the Hoover algorithm<sup>32</sup>), first at 1000 K, then at 600 K, and finally at the desired temperature, at least for 200 ps at each stage, keeping an external pressure of 1 bar. This equilibration scheme is inspired by the procedure followed by Del Popolo et al.<sup>33</sup> The molar volumes obtained are listed in Table 2. The systems were further equilibrated by velocity

rescaling at constant volume and temperature for at least an additional 200 ps interval. Finally, the production runs were obtained in the NVE ensemble. Shear viscosities were obtained from trajectories of 8 ns, for which the components of the stress tensor were recorded in intervals of 20 fs. For the calculation of self-diffusion and conductivity, shorter runs (800 ps) were employed, with position and velocity of all particles being recorded every 40 fs. Note that the dynamics of these systems is further more complex than that of simple fluids; this implies slow decays in the correlation functions. We have performed some preliminary tests on the effect of the time resolution in the damped trajectory on the accuracy of the running integral of the corresponding transport coefficients. Our results indicated that the convergence values of the integral obtained with the 40 fs time resolution agreed almost exactly with the integral calculated with the maximum time resolution for the diffusion coefficient, while similar conclusions were obtained for a resolution of 20 fs and the shear viscosities.

The equations of motion were integrated through the Verlet and Fincham's implicit quaternion algorithms as implemented in the DL\_POLY package (version 2.13),<sup>34,35</sup> with a constant time step of 0.002 ps. This time step provided a good energy conservation with small fluctuations, with the relative drift in the total energy being less than  $2 \cdot 10^{-5}$  in 4 ns.

The Coulombic interactions were evaluated through the Ewald method using the convergence parameter ( $\alpha$ ) and the largest reciprocal space vector ( $k_{\text{max}}$ ) that yielded a relative accuracy of  $1 \cdot 10^{-5}$  in the electrostatic energy.<sup>35</sup> The accuracy of the Ewald sum was checked by comparison of the estimated Coulombic energy and the Coulombic virial in absolute value. The real space force cutoff for both the LJ and Coulomb pair interactions was taken as 15 Å for all the system sizes, except for the smallest (64 ion pairs), where a cutoff of 12 Å was taken. Long-range corrections to the potential energy and virial of the system were applied.

### 3. Results and Discussion

The values of the average temperature and molar volume used in the 8 ns simulations of 125 ion pairs are provided in Table 2. The molar volumes are larger than the values extrapolated from experimental data in the range 300–366 K<sup>36</sup> by 5–8%. This accuracy in density is similar to the results reported by Hanke et al.<sup>12</sup> for [mmim]Cl using an equivalent molecular model. The temperature dependence of the volume is linear to a good approximation, and the computed isobaric volume expansivity, calculated as the slope of the plot  $V_M$  vs  $T$ , is lower than the experimental value by ca. 20%. This level of agreement is quite good, considering that none of the force field parameters have been optimized to match experimental data.<sup>28</sup> Comparable agreement on the volumetric expansivity between simulation results and experimental values has been reported with more refined force fields for different ILs.<sup>37,38</sup>

The average intermolecular contribution to the potential energy, which includes electrostatic and van der Waals interactions, is also reported in Table 2. The results indicate that the electrostatic contribution is the most important one, in agreement with other simulation studies.<sup>12,37</sup> The intermolecular energies agree very well with the values reported by Urahata and Ribeiro (using a similar set of partial atomic charges) for [emim]Cl.<sup>31</sup> They are also comparable to those of other ILs and considerably larger than volatile organic compounds.

**A. Effect of the System Size.** A key parameter when performing extensive computer simulations as the ones reported here is the system size; it is essential to estimate the smaller size of the system which allows the calculation of the relevant properties with enough accuracy and reasonable CPU cost.



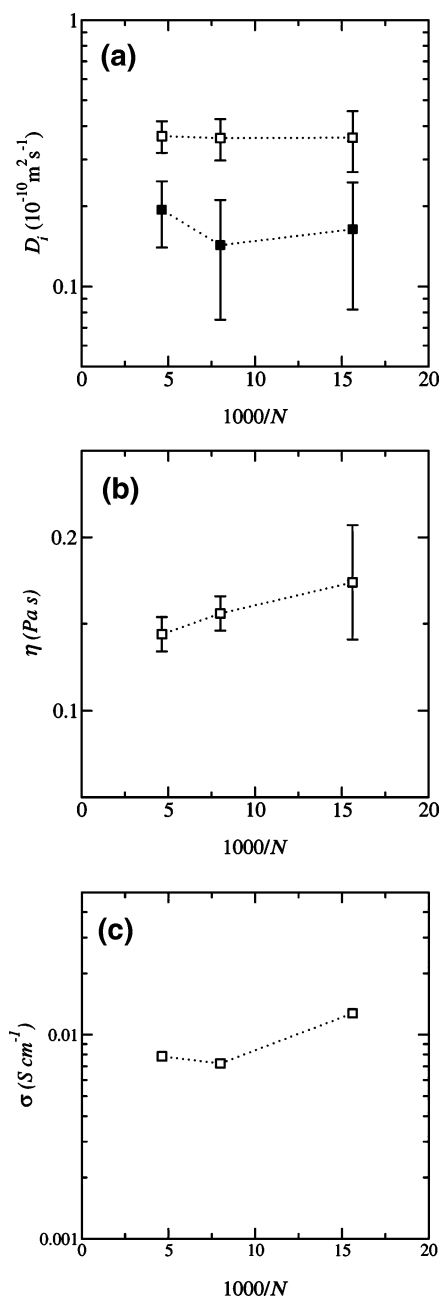


**Figure 2.** Effect of system size on the transport properties of [emim]-Cl estimated from MD simulations at 400 K and 1 bar. (a) Self-diffusion coefficients of  $\text{emim}^+$  (open symbols) and  $\text{Cl}^-$  (solid symbols). (b) Shear viscosity (the data were corrected for the small differences in the average temperature among the different NVE simulations, using the relationship observed as a function of  $T$ ). (c) Electrical conductivity (uncertainties are on the order of  $0.01 \text{ S cm}^{-1}$ ).

Hence, we have first analyzed the influence of the number of ion pairs in the system,  $N$ , on the estimated transport parameters, to check that no drastic finite size effects would affect our calculations. Figure 2 shows the results for self-diffusion coefficients, shear viscosity, and electrical conductivity obtained with systems of 64, 125, and 216 ion pairs at 400 K. Although the statistical uncertainty is somewhat improved as the system size increases, no clear trend in the average values with the number of molecules can be assessed from these results. A very small influence of the system size on the viscosity have also been observed in MD simulations of LJ fluids.<sup>22,24,39</sup>

**B. Self-Diffusion Coefficients.** The self-diffusion coefficients at temperatures  $T = 380, 404, 450$ , and  $486 \text{ K}$  have been calculated from the Green–Kubo relations. As a representative

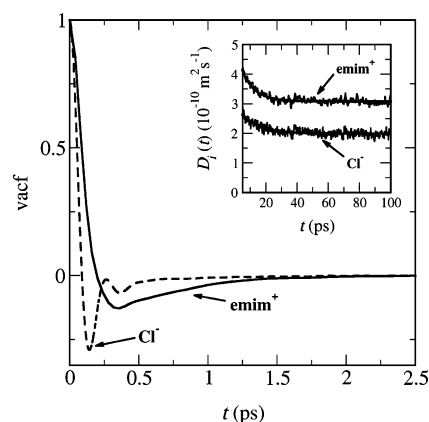


**Figure 3.** Normalized velocity autocorrelation functions ( $\text{vacf}$ ) of  $\text{emim}^+$  and  $\text{Cl}^-$  obtained at 486 K and 1 bar. The inset shows the running integral, eq 1, representing the self-diffusion coefficients of cation and anion (gray line), together with the best-fit exponential decay function, eq 2 (black line).

example of the results obtained, the velocity autocorrelation functions ( $\text{vacf}$ ) of the cation and anion in [emim]Cl at 486 K are shown in Figure 3. It can be seen that the autocorrelation function of the cation decays quickly, reaching a zero value at ca. 0.2 ps and then a negative asymptotic plateau up to 2 ps. No long-time tails are noticeable. The position of the first zero represents the average collision time due to the “cage” effect, typical of condensed phases, and it agrees very well with results from other simulations of ILs.<sup>33</sup> In the case of the anion, however, the  $\text{vacf}$  decays even more quickly and shows an oscillatory behavior similar to that of rigid-ion models of inorganic molten salts<sup>23,40</sup> (see also Figure 1). This behavior has been interpreted as a “rattling” motion of the lighter ion inside a relatively long-lived cage formed by the heavier counterions.<sup>33,41</sup> In contrast with this, simulation results for [emim] $\text{NO}_3$  (which presents a smaller difference in weight between both ions) do not yield such marked oscillations in the correlation function of the anion.<sup>33</sup> Comparisons of the normalized  $\text{vacf}$  functions for the four temperatures under study do not show significant differences.

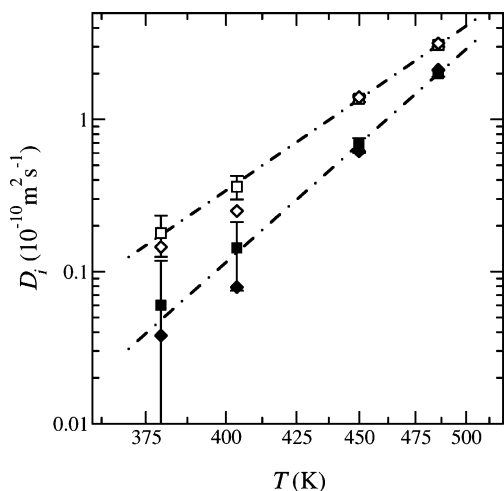
The diffusion coefficients of the ions were calculated from the time integrals of the  $\text{vacf}$ , as explained in the previous section. As can be seen in the inset of Figure 3, the running integrals reach a plateau within 100 ps, from which the self-diffusion coefficients are calculated (Table 3). This coefficient is larger for the cation at all the temperatures studied, in apparent contradiction to its larger size and mass compared to the  $\text{Cl}^-$  ion. The fact that the lighter anions have smaller diffusion coefficients has also been observed experimentally,<sup>1</sup> and it has been attributed to the smaller hindrance of the cation motion along the direction perpendicular to the nitrogen atoms on the ring plane.<sup>41</sup> Comparison with results from MD simulations using different interaction potentials shows that flexible models and/or explicit atom models predict somewhat larger diffusion constants.<sup>12,16</sup>

Figure 4 depicts the self-diffusion coefficients at different temperatures as obtained from the Green–Kubo relation. Results obtained from the Einstein relation are also shown for comparative purposes. As expected, both methods give similar results, with the calculated values agreeing in all cases within statistical uncertainties; the agreement improves at high temperatures, where the statistical accuracy is also larger. Regarding the behavior of the diffusion coefficient, it is observed that its value increases with temperature, as expected. The good linear behavior of  $\log D_i$  vs  $1/T$  indicates that the temperature dependence of the diffusion coefficients can be expressed

**TABLE 3: Diffusion Coefficients, Electrical Conductivities, and Shear Viscosities Calculated from MD Simulations of [emim]Cl at Different Temperatures<sup>a</sup>**

$T$ (K)	$D_{\text{anion}}$ ( $10^{-10} \text{ m}^2 \text{ s}^{-1}$ )	$D_{\text{cation}}$ ( $10^{-10} \text{ m}^2 \text{ s}^{-1}$ )	$\sigma$ ( $10^{-3} \text{ S cm}^{-1}$ )	$\sigma_{\text{NE}}$ ( $10^{-3} \text{ S cm}^{-1}$ )	$T$ (K)	$\eta$ (Pa s)
380	0.60 (0.58)	1.79 (0.54)	4.7 (10)	4.9 (2.3)	378	0.47 (0.22)
404	1.43 (0.68)	3.61 (0.64)	7.2 (11)	9.6 (2.5)	395	0.20 (0.05)
450	6.77 (0.76)	13.7 (0.7)	41 (11)	35 (2)	444	0.032 (0.010)
486	20.0 (0.9)	30.8 (0.8)	85 (31)	77 (3)	489	0.014 (0.005)

<sup>a</sup> The conductivities calculated from the Nernst–Einstein relation ( $\sigma_{\text{NE}}$ ) are also listed for comparison. Uncertainties are given in brackets.



**Figure 4.** Self-diffusion coefficients of  $\text{emim}^+$  (open squares) and  $\text{Cl}^-$  (solid squares), calculated from the Green–Kubo relation, as a function of the temperature. Values obtained from the Einstein relation are also shown, for comparison purposes (open and solid diamonds). The dotted–dashed line corresponds to the least-squares fit of an empirical Arrhenius relationship, eq 13, from the slope of which the activation energies have been estimated.

**TABLE 4: Activation Energies Obtained from Arrhenius Plots of the Transport Coefficients Calculated from MD Simulations over the Temperature Range 378–489 K and Comparison with Experimental Data**

$E_{D,\text{emim}^+}^\ddagger$ (kJ mol <sup>-1</sup> )	$E_{D,\text{Cl}^-}^\ddagger$ (kJ mol <sup>-1</sup> )	$E_\eta^\ddagger$ (kJ mol <sup>-1</sup> )	$E_\sigma^\ddagger$ (kJ mol <sup>-1</sup> )
41 <sup>a</sup>	51 <sup>a</sup>	49 <sup>a</sup>	44 <sup>a</sup>
		52 <sup>b</sup>	42 <sup>c</sup>

<sup>a</sup> This work. <sup>b</sup> Calculated from experimental data reported by Seddon et al.<sup>8</sup> in the range 323–363 K. <sup>c</sup> Calculated from experimental data of Fannin et al.<sup>36</sup> in the range 325–383 K.

through an empirical Arrhenius equation, i.e.,

$$D_i = D_{i,0} \exp\left(-\frac{E_D^\ddagger}{RT}\right) \quad (13)$$

where  $E_D^\ddagger$  is regarded as an activation energy for self-diffusion.

The values of  $E_D^\ddagger$  are listed in Table 4. Note that the activation energy for the self-diffusion of the anion is greater than for the cation, which is due to the fact that the former is on average in a deeper potential well compared to the cation, as observed in MD simulations of [mmim]Cl.<sup>16</sup>

**C. Shear Viscosity.** The running integral for the shear viscosity of [emim]Cl at 444 K is represented in Figure 5. The inset shows the average normalized autocorrelation function of the six independent components of the pressure tensor. It can be noted that the fluctuations in the pressure tensor decay very slowly and vanish only after around 0.5–1 ns. This time correlation function shows two characteristic decay times, namely, a very fast relaxation in the subpicosecond time scale,

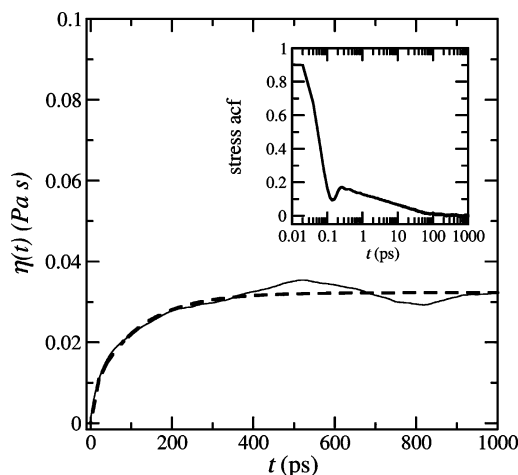


**Figure 5.** Running integral, eq 3, corresponding to the shear viscosity of [emim]Cl at 444 K and 1 bar (thin line) and the best-fit empirical function used for the estimation of the extrapolated value, eq 5 (thick dashed line). The inset shows the normalized stress tensor autocorrelation function on a logarithmic time scale.

and a long-time component that decays on a scale of hundreds of picoseconds. The initial fast relaxation takes place approximately on the same time scale as the decay of the translational velocity correlation function of the ions, whereas the subsequent slow relaxation has a decay time on the same order of magnitude as the reorientation of the imidazolium ring, which is relatively slow.<sup>33,41</sup> Accordingly, the running integral of the viscosity reaches a plateau only after around 1000 ps or more, depending on the temperature. The fit to the empirical double-decay function, eq 5, is quite satisfactory and allows the estimation of an extrapolated value for the shear viscosity. However, the statistical accuracy of the viscosity is not as good as for the self-diffusion, due to the fact that the former is a collective dynamical property.

Figure 6 depicts a comparison between simulated and experimental values<sup>8</sup> of the shear viscosity at different temperatures. It is clearly observed that MD simulations performed with this model overestimate this property by ca. 1 order of magnitude. It must be pointed out that the experimental results of Seddon et al.<sup>8</sup> are reported as preliminary data, since they correspond to samples of [emim]Cl with relatively high contents of impurities such as water, and the values corresponding to the “pure” compound are expected to be somewhat larger. Moreover, these results were obtained at temperatures below the melting point of 360 K reported for [emim]Cl,<sup>1</sup> and therefore, they correspond to a glassy state of the ionic liquid. Hence, the simulation results are relatively satisfactory, if we take into account the simplicity of the force field employed for this study. As stated, this model is based on a very general force field,<sup>28</sup> and it has not been optimized with respect to experimental transport properties. The use of flexible and/or all-atom models could improve the viscosity estimates, although a comparison with other simulation results indicate that this is probably not the major source of discrepancy with experiments. For instance,

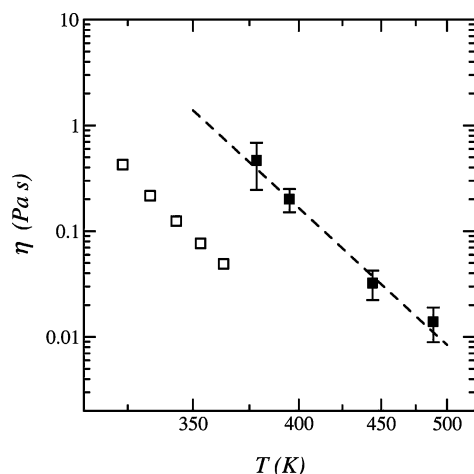


**Figure 6.** Shear viscosity of [emim]Cl as a function of the temperature, estimated from MD simulation (solid symbols). The dashed line corresponds to the least-squares fit of an empirical Arrhenius equation. Some experimental values taken from Seddon et al.<sup>8</sup> (open symbols) are shown for comparison. It must be mentioned that the authors report high impurity contents for their samples, so their results should be regarded as preliminary data.

the fully flexible model of Canongia Lopes et al.<sup>14</sup> leads to a value for the viscosity of [mmim]Cl (slightly smaller in size than [emim]Cl) of 0.048 Pa·s at 425 K,<sup>16</sup> which matches very well with the value interpolated at the same temperature from the results of this work (see Figure 6). Moreover, the consideration of electronic polarizability in the molecular force field has been proven to represent a significant difference in both diffusion constants and viscosity, in much better agreement with experimental results.<sup>17</sup> The effect of polarizability is to make ions more mobile by decreasing or “damping” the oscillations in the velocity autocorrelation function and therefore enhancing the diffusion coefficients. In a rigid ion model, the constraint of local charge neutrality hinders the displacement of a particular ion with respect to its neighboring counterions, while for polarizable ions, additional screening can be provided by the dipolar moments induced in the surrounding ions.<sup>23</sup> A similar effect on the stress relaxation and, therefore, on the calculated viscosity is expected. As a result, the effect of accounting for polarizability in the molecular model appears similar to increasing the temperature in a nonpolarizable model.<sup>17</sup> In other words, the effect of polarizability would probably represent a “shift” in the  $\eta$  vs  $T$  curve of Figure 6 toward the left.

It should be emphasized that, despite the noticeable difference in absolute value, the simulation results reproduce very well the trend in the experimental viscosity with temperature. In both cases, a good linear relationship  $\log \eta$  vs  $T^{-1}$  is observed, with a good agreement on the slopes. The estimated activation energy is quite close to the value calculated from experimental data at lower temperature (Table 4). It is also close to the values observed for other dialkylimidazolium halides such as [mpim]-Br,<sup>42</sup> although it is quite high compared to ILs of [emim]<sup>+</sup> with fluoroanions derived from borate, for which  $E_{\eta}^{\ddagger}$  lies in the range 28–36 kJ·mol<sup>-1</sup>.<sup>43</sup> The activation energy of [emim]Cl is particularly high compared to most conventional molecular liquids and molten salts, which usually follow the empirical relationship  $E_{\eta}^{\ddagger} = 3.74RT_m$ ,<sup>44</sup> where  $T_m$  is the melting temperature. In this way, the experimental melting point of [emim]Cl would correlate with an activation energy of 11 kJ mol<sup>-1</sup>. The reason for the high energy observed is probably connected with the existence of a glassy state.

**D. Electric Conductivity and Correlation among Transport Coefficients.** The time correlation function of the electric

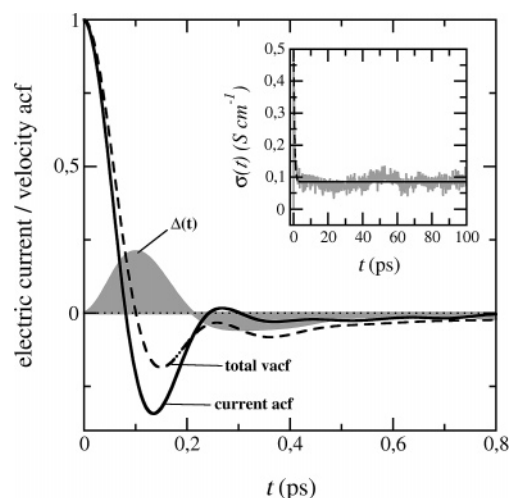


**Figure 7.** Normalized electric current autocorrelation function of [emim]Cl at 486 K and 1 bar (bold solid line); total velocity autocorrelation function (dashed line); and difference between them,  $\Delta(t)$ , indicating the degree of cross-correlation among ions (shaded in gray). The inset shows the running integral eq 7 representing the electrical conductivity (gray line), together with the best-fit exponential decay function (black line).

current is shown in Figure 7. It can be noted that the current fluctuations decay very quickly and vanish within 1 ps. The time integral of the correlation function is affected by relatively large statistical noise (see inset of the figure), and therefore, the accuracy in the estimated values of the electrical conductivity is rather small, particularly at the two lowest temperatures (at which the estimated uncertainties are on the same order of  $\sigma$ ). Again, comparison with experimental conductivity data<sup>36</sup> reveals only qualitative agreement. For instance, the value of  $\sigma$  at 380 K, interpolated from the data reported by Fannin and co-workers, is 0.034 S·cm<sup>-1</sup>.

Despite the relatively high uncertainty in the conductivities estimated from integration of the charge current correlation function, a good linear  $\log \sigma$  vs  $T^{-1}$  is observed (see Figure 8), in a similar way as with the other transport coefficients. Again, the activation energy compares very well with experimental activation energy at lower temperatures<sup>36</sup> (see Table 4). It is also slightly lower than the activation energy for viscous flow, a relation that also holds for experimental results of [emim]Cl, other [emim]<sup>+</sup> ILs<sup>43,45</sup> and inorganic molten salts.<sup>44</sup>

The mechanism of charge transport in these systems is related with the process of self-diffusion of the ions. In fact, an expression for the electric conductivity as a function of the diffusion coefficients of cation and anion can be derived from eqs 7 and 8. If the cross terms ( $i \neq j$ ) are negligible in the current autocorrelation function, then the Nernst–Einstein equation is obtained<sup>23,44</sup>

$$\sigma = \frac{e^2}{k_B T} \sum_i \rho_i q_i D_i \quad (14)$$

where  $e$  is the electric charge unit,  $\rho$  and  $q$  are the molar density and charge of the ions, respectively, and  $i$  denotes cation or anion. The deviations from eq 14 are interpreted in terms of cross-correlations among ions.<sup>23,44</sup> Thus, if the ratio between the experimental value of  $\sigma$  and the conductivity calculated from eq 14 is smaller than unity, then a significant fraction of oppositely charged ions are moving together in the time scale of diffusive motion. The motion of these neutral, short-lived ion clusters contributes therefore to self-diffusion but not to the net charge transport. Such correlated motions do not necessarily

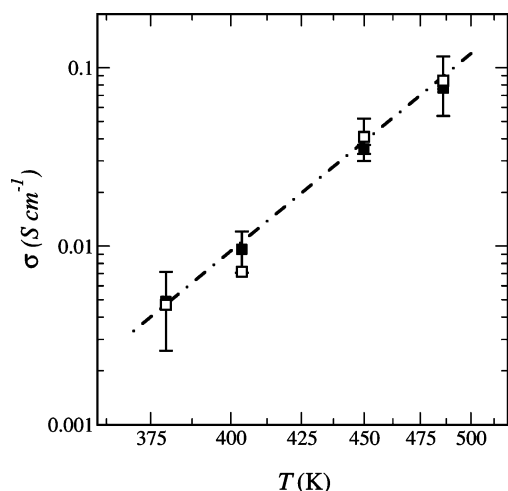


**Figure 8.** Electrical conductivity of [emim]Cl as a function of the temperature, calculated from the electric current acf and Green–Kubo relation (open symbols), and from the diffusion coefficients through Nernst–Einstein equation (solid symbols). The dotted–dashed line corresponds to the least-squares fit of an empirical Arrhenius equation. The estimated uncertainties of the open symbols at the two lowest temperatures are on the same order of magnitude as the values themselves and are not shown. The error bars of the Nernst–Einstein values at the two highest temperatures are smaller than the symbol size.

involve the existence of actually bonded pair species, even on a transient basis. Ratios of this kind, calculated from experimental impedance and NMR experimental data on ILs, are usually smaller than 1, depending on the particular IL and temperature.<sup>10,46</sup> For instance, ratios between experimental and Nernst–Einstein conductivities of 0.6–0.8 have been reported for [emim]Br and [emim]I over the range 243–403 K.<sup>10</sup> This suggests that “ion pairing” (or rather, cross-correlations among cations and anions) can take place in ILs to some extent. It is interesting to note that, although the presence of water impurities increases notably both the diffusion coefficients and the conductivity, it has little effect on the ratio between experimental and Nernst–Einstein conductivities, suggesting that the ion association remains virtually unaffected.<sup>47</sup>

The values of the conductivity estimated using the Nernst–Einstein equation with the diffusion coefficients obtained from the MD simulations are shown in Figure 8, together with the results calculated from Green–Kubo. It is clear that both sets of data agree within their respective errors. It can be concluded that the molecular model used in this work does not lead to a significant overall cross-correlation among ions, and therefore, cation and anion behave as independent ions regarding diffusion and charge transport. However, the differences between the conductivity and the Nernst–Einstein value observed experimentally are comparable with the statistical uncertainty in the simulation results.

The relevance of correlations among ions of the same and opposite charges can be seen more clearly in the difference between the electric current correlation and the total velocity autocorrelation functions<sup>23,33,40</sup> (see Figure 7). If these cross-correlations were negligible, then the ions would behave independently, and the normalized curves of  $\vec{v}(t_0 + t) \cdot \vec{v}(t_0)$  and  $\vec{J}(t_0 + t) \cdot \vec{J}(t_0)$  correlation functions would coincide. At very short times, however, the current correlation function decays faster than the total *vacf*, which means that some of the ions diffuse together with their oppositely charged neighbors and do not contribute to charge transport. These cation–anion associations are short-lived and unstable, with lifetimes of around 0.1 ps, in agreement with simulation results from [emim]-

NO<sub>3</sub><sup>33</sup> and molten inorganic salts such as NaCl.<sup>40</sup> At slightly longer times, however, the difference between both correlation functions becomes negative, indicating that the effects of correlations between different ions of the same sign can also be significant. Eventually, both effects probably cancel each other, and hence, the overall effect of cross-correlations would be negligible. This would explain the good agreement of the conductivity calculated from Green–Kubo with the value obtained from the diffusion coefficients through the Nernst–Einstein relation (Figure 8).

An increasing interest is appearing in the literature concerning the relationship between conductivity and fluidity in ILs. In these systems (and, more generally, in electrolyte solutions), the conductivity is often found to be inversely proportional to viscosity,<sup>1,9,44</sup> a behavior that is usually called Walden’s rule

$$\Lambda\eta = \text{constant} \quad (15)$$

where  $\Lambda$  is the molar conductivity

$$\Lambda = \frac{\sigma M}{\rho} \quad (16)$$

and  $\sigma$ ,  $M$ , and  $\rho$  are the electrical conductivity (S·m<sup>−1</sup>), molecular weight, and density, respectively. Ideally, the Walden product is independent of the temperature for a given IL. The goodness of fit of this linear relationship to data from a wide range of ILs and different temperatures is remarkable (see, for instance, Figure 3.6–4 in the review of Trulove and Mantz<sup>1</sup>). Furthermore, the values of the Walden product have been found to be fairly independent of the presence of traces of water.<sup>48</sup> However, relatively small to significant variations in the Walden products with temperature have recently been described in ILs based on alkyl/arenyltrifluoroborate anions.<sup>43</sup> The experimental fulfillment of eq 15 indicates that the density of mobile charge carriers in an IL is strongly correlated with its viscosity.

The Walden’s rule can be derived from the combination of eqs 14 and 16 with the Stokes–Einstein relation

$$D_i = \frac{k_B T}{c\pi\eta r_i} \quad (17)$$

where  $k_B$  is Boltzmann’s constant,  $T$  is the absolute temperature,  $c$  is a constant (4–6), and  $r_i$  is the effective hydrodynamic radius of the ion. The latter is an effective radius that takes solvation and coordination into account, and it gives an indication of the degree of association between ions. In this way, as the interaction of the ion with its neighboring counterions becomes stronger, its behavior resembles more that of a coordinated complex than a free ion (in the time scale of the diffusive motion), and consequently, the hydrodynamic radius increases.<sup>49</sup> Good linear relationships between  $1/D$  and  $\eta/T$  have been found experimentally, for instance, in the IL [bmim][PF<sub>6</sub>].<sup>11</sup> Note that, if Stokes–Einstein and Nernst–Einstein apply, the effect of temperature cancels out, and hence, the value of the constant in eq 15 would only depend on the hydrodynamic radii of the ions.

The Walden plots have been recently proposed as a basis for a general rationalization of the experimental behavior of charged fluids. Following the ideas of Angell and co-workers,<sup>9,50</sup> the ILs that more closely follow the Walden plot usually display ideal behavior, with no correlation among ions and very low vapor pressure. On the contrary, molten salts with conductivities below the values predicted by this relationship show an important influence of ion pairing and higher vapor pressures. In contrast, the combination of high conductivities and low



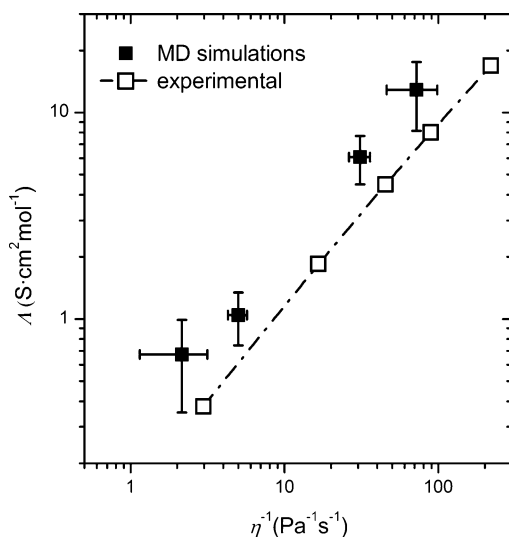


**Figure 9.** Walden plot of the molar conductivity and shear viscosity calculated from MD simulations of [emim]Cl at different temperatures (solid symbols). For the points at the two lowest temperatures, the error bars in  $\Lambda$  were calculated from the uncertainties in the diffusion coefficients. The open symbols were calculated from the experimental conductivities and viscosities reported by Fannin et al.<sup>36</sup> and Seddon et al.,<sup>8</sup> respectively.

fluidities is characteristic of superionic glasses. In all these cases, the slope of  $\log \Lambda$  vs  $\log \eta^{-1}$  has a value between 1 and 0.

The fulfillment of Walden's rule in the MD simulation results is represented in Figure 9. As can be seen, a good linear relationship  $\log \Lambda$  vs  $\log \eta^{-1}$  is obtained, with a slope of 0.9, very close to the theoretical value of 1, and in excellent agreement with experimental results. Two main conclusions can be extracted from these results. First, the simulations anticipate the good fulfillment of Walden's rule of the experimental [emim]Cl. Therefore, the degree of ion pairing, whether it is significant or not, do not seem to vary considerably with temperature (or, at least, its effect cancels out with changes in the hydrodynamic radius). Nevertheless, deviations from the Walden's rule with temperature have been reported for other imidazolium ILs,<sup>43</sup> which suggests that the behavior of [emim]Cl might not be representative of this class of ILs. Second, the discrepancy in the intercept of the Walden plots from experimental and simulation data can tentatively be ascribed to differences in the hydrodynamic radius between the model and the experimental system, provided that Nernst–Einstein and Stokes–Einstein apply. In this case, it would be worthwhile to carry out a comparison of the relaxation time scale of the coordination shells of cation and anion in the bulk IL with the structural relaxation time of the solvent, in a similar way as the recent work of Madden and co-workers with molten alkali halides.<sup>49</sup> This study would provide a more detailed insight into the dynamics of ion association, and it could also be a good test to prove the reliability of different force fields in the description of the transport properties of experimental ILs and their mixtures with different solutes.

#### 4. Closing Remarks

The aim of this study was to analyze the ability of a simple molecular model of an IL to describe the behavior of some transport properties of [emim]Cl as a function of the temperature as well as their mutual relationships, through MD simulations. The model predictions of the transport coefficients are relatively rough compared with experimental data, and yet, these results are noteworthy, taking into account that the force field has not been optimized with respect to any macroscopic transport

property of the system under study. As stated by Yan et al.,<sup>17</sup> the inclusion of the electronic polarizability in the model should lead to much better agreement with experimental viscosities, with a similar effect on the estimated properties as an increase of temperature in the nonpolarizable model. Nevertheless, the simulations allow a successful estimation of the activation energies.

From the point of view of diffusion and charge transport, the molecular model used in this work does not seem to predict an important degree of ion association, except on a very short time scale. Moreover, the simulations reproduce remarkably well the slope of the Walden plots obtained from experimental data of [emim]Cl, confirming that temperature does not alter appreciably the extent of ion pairing. However, further studies on the dynamics of relaxation of the solvation shells are suggested in order to corroborate these conclusions. It would also be interesting to explore whether other force fields for [emim]Cl more refined than the nonpolarizable, rigid, united atom model used in this work will lead to a different description of the collective dynamics of cations and anions in the melt. In particular, it can be anticipated that the inclusion of electronic polarizability would probably lead to greater Nernst–Einstein deviation factors, in better agreement with experiment.

This work presents the first results of an ongoing project on the study of the relationship among molecular structure and transport/equilibrium properties through molecular modeling tools.

**Acknowledgment.** The authors would like to thank W. Smith for kindly providing the DL\_POLY source code. Helpful discussions with A. Mejía, A. Olivet, and A. Lozano are gratefully acknowledged. Partial financial support for this work has been provided by the Spanish government under project no. CTQ2005-00296/PPQ and by the Generalitat de Catalunya (SGR2005-00288). C. Rey-Castro acknowledges an I3P (CSIC) postdoctoral research contract from the Spanish Government (Ministerio de Educación y Ciencia) cofunded by the European Social Fund, EU. This research has been carried out partially using computational resources from CESCA (Catalunya, Spain).

#### References and Notes

- (1) Wasserscheid, P.; Welton, T., Eds. *Ionic Liquids in Synthesis*; Wiley-VCH: Weinheim, 2003.
- (2) Rogers, R. D.; Seddon, K. R., Eds. *Ionic Liquids: Industrial Applications for Green Chemistry*; American Chemical Society: Washington, DC, 2002; Vol. 818.
- (3) Rogers, R. D.; Seddon, K. R., Eds. *Ionic Liquids as Green Solvents: Progress and Prospects*; American Chemical Society: Washington, DC, 2003; Vol. 856.
- (4) Rogers, R. D.; Seddon, K. R., Eds. *Ionic Liquids IIIA: Fundamentals, Progress, Challenges and Opportunities. Properties and Structure*; American Chemical Society: Washington, DC, 2005; Vol. 901.
- (5) Rogers, R. D.; Seddon, K. R., Eds. *Ionic Liquids IIIB: Fundamentals, Progress, Challenges and Opportunities. Transformations and Processes*; American Chemical Society: Washington, DC, 2005; Vol. 902.
- (6) Anthony, J. L.; Maginn, E. J.; Brennecke, J. F. *J. Phys. Chem. B* **2002**, *106*, 7315.
- (7) Chiappe, C.; Pieraccini, D. *J. Phys. Org. Chem.* **2005**, *18*, 275.
- (8) Seddon, K. R.; Stark, A.; Torres, M. J. In *Clean Solvents: alternative media for chemical reactions and processing*; Abraham, M. A., Moens, L., Eds.; American Chemical Society: Washington, DC, 2002; Vol. 819, p 34.
- (9) Xu, W.; Cooper, E. I.; Angell, C. A. *J. Phys. Chem. B* **2003**, *107*, 6170.
- (10) Every, H. A.; Bishop, A. G.; MacFarlane, D. R.; Oradd, G.; Forsyth, M. *Phys. Chem. Chem. Phys.* **2004**, *6*, 1758.
- (11) Umecky, T.; Kanakubo, M.; Ikushima, Y. *Fluid Phase Equilib.* **2005**, *228*, 329.
- (12) Hanke, C. G.; Price, S. L.; Lynden-Bell, R. M. *Mol. Phys.* **2001**, *99*, 801.
- (13) de Andrade, J.; Boes, E. S.; Stassen, H. In *Ionic Liquids IIIA: Fundamentals, Progress, Challenges, and Opportunities. Properties and*

Structure; Rogers, R. D., Seddon, K. R., Eds.; American Chemical Society: Washington, DC, 2005; Vol. 901, p 118.

(14) Lopes, J. N. C.; Deschamps, J.; Padua, A. A. H. *J. Phys. Chem. B* **2004**, *108*, 2038.

(15) Lopes, J. N. C.; Deschamps, J.; Padua, A. A. H. In *Ionic Liquids IIIA: Fundamentals, Progress, Challenges, and Opportunities. Properties and Structure*; Rogers, R. D., Seddon, K. R., Eds.; American Chemical Society: Washington, DC, 2005; Vol. 901, p 134.

(16) Bhargava, B. L.; Balasubramanian, S. *J. Chem. Phys.* **2005**, *123*, 144505.

(17) Yan, T. Y.; Burnham, C. J.; Del Popolo, M. G.; Voth, G. A. *J. Phys. Chem. B* **2004**, *108*, 11877.

(18) Wu, X. P.; Liu, Z. P.; Huang, S. P.; Wang, W. C. *Phys. Chem. Chem. Phys.* **2005**, *7*, 2771.

(19) Lee, S. U.; Jung, J.; Han, Y. K. *Chem. Phys. Lett.* **2005**, *406*, 332.

(20) Allen, M. P.; Tildesley, D. J. *Computer Simulation of Liquids*; Oxford University Press: New York, 1987.

(21) Frenkel, D.; Smit, B. *Understanding Molecular Simulation. From algorithms to applications*, 2nd ed.; Academic Press: New York, 2002.

(22) Haile, J. M. *Molecular Dynamics Simulation. Elementary methods*; John Wiley & Sons: New York, 1992.

(23) Hansen, J. P.; McDonald, I. R. *Theory of Simple Liquids*; Academic Press: New York, 1986.

(24) Holian, B. L.; Evans, D. J. *J. Chem. Phys.* **1983**, *78*, 5147.

(25) Hess, B. *J. Chem. Phys.* **2002**, *116*, 209.

(26) Fumi, F. G.; Tosi, M. P. *J. Phys. Chem. Solids* **1964**, *25*, 31.

(27) Tosi, M. P.; Fumi, F. G. *J. Phys. Chem. Solids* **1964**, *25*, 45.

(28) Shim, Y.; Choi, M. Y.; Kim, H. J. *J. Chem. Phys.* **2005**, *122*, 044510.

(29) Elaiwi, A.; Hitchcock, P. B.; Seddon, K. R.; Srinivasan, N.; Tan, Y. M.; Welton, T.; Zora, J. A. *J. Chem. Soc., Dalton Trans.* **1995**, 3467.

(30) Cornell, W. D.; Cieplak, P.; Bayly, C. I.; Gould, I. R.; Merz, K. M.; Ferguson, D. M.; Spellmeyer, D. C.; Fox, T.; Caldwell, J. W.; Kollman, P. A. *J. Am. Chem. Soc.* **1995**, *117*, 5179.

(31) Urahata, S. M.; Ribeiro, M. C. C. *J. Chem. Phys.* **2004**, *120*, 1855.

(32) Melchionna, S.; Ciccotti, G.; Holian, B. L. *Mol. Phys.* **1993**, *78*, 533.

(33) Del Popolo, M. G.; Voth, G. A. *J. Phys. Chem. B* **2004**, *108*, 1744.

(34) Smith, W.; Yong, C. W.; Rodger, P. M. *Mol. Simul.* **2002**, *28*, 385.

(35) Smith, W.; Forester, T. R. *The DL\_POLY Molecular Simulation Package*, v. 2.13; 1999. Daresbury Laboratory, U.K.; [http://www.cse.clrc.ac.uk/msi/software/DL\\_POLY/](http://www.cse.clrc.ac.uk/msi/software/DL_POLY/).

(36) Fannin, A. A.; Floreani, D. A.; King, L. A.; Landers, J. S.; Piersma, B. J.; Stech, D. J.; Vaughn, R. L.; Wilkes, J. S.; Williams, J. L. *J. Phys. Chem.* **1984**, *88*, 2614.

(37) Morrow, T. I.; Maginn, E. J. *J. Phys. Chem. B* **2002**, *106*, 12807.

(38) Cadena, C.; Zhao, Q.; Snurr, R. Q.; Maginn, E. J. *J. Phys. Chem. B* **2006**, *110*, 2821.

(39) Meier, K.; Laesecke, A.; Kabelac, S. *J. Chem. Phys.* **2004**, *121*, 3671.

(40) Trullas, J.; Padro, J. A. *Phys. Rev. B* **1997**, *55*, 12210.

(41) Urahata, S. M.; Ribeiro, M. C. C. *J. Chem. Phys.* **2005**, *122*, 024511.

(42) Jarosik, A.; Krajewski, S. R.; Lewandowski, A.; Radzinski, P. *J. Mol. Liq.* **2006**, *123*, 43.

(43) Zhou, Z. B.; Matsumoto, H.; Tatsumi, K. *Chemphyschem* **2005**, *6*, 1324.

(44) Bockris, J. O. M.; Reddy, A. K. N. *Modern Electrochemistry*, 2nd ed.; Plenum Press: New York, 1998; Vol. 1.

(45) Hayamizu, K.; Aihara, Y.; Nakagawa, H.; Nukuda, T.; Price, W. S. *J. Phys. Chem. B* **2004**, *108*, 19527.

(46) Noda, A.; Hayamizu, K.; Watanabe, M. *J. Phys. Chem. B* **2001**, *105*, 4603.

(47) Kanakubo, M.; Umecky, T.; Aizawa, T.; Kurata, Y. *Chem. Lett.* **2005**, *34*, 324.

(48) Widegren, J. A.; Saurer, E. M.; Marsh, K. N.; Magee, J. W. *J. Chem. Thermodyn.* **2005**, *37*, 569.

(49) Brookes, R.; Davies, A.; Ketwaroo, G.; Madden, P. A. *J. Phys. Chem. B* **2005**, *109*, 6485.

(50) Yoshizawa, M.; Xu, W.; Angell, C. A. *J. Am. Chem. Soc.* **2003**, *125*, 15411.

(51) Galamba, N.; de Castro, C. A. N.; Ely, J. F. *J. Phys. Chem. B* **2004**, *108*, 3658.

(52) Koishi, T.; Tamaki, S. *J. Non-Cryst. Solids* **1999**, *252*, 501.